

<sup>1</sup>. Dana-Mirela COSTEA, <sup>2</sup>. Mugurel-Nicolae GĂMAN, <sup>3</sup>. George DUMITRU

## CONSIDERATIONS ON TRIBOLOGICAL PHENOMENONS AT THE WHEEL- RAIL CONTACT LEVEL, SPECIFIC TO THE BR 189 CLASS LOCOMOTIVES

<sup>1</sup>. UPB, ROMANIAN RAILWAY AUTHORITY - AFER, ROMANIA

<sup>2-3</sup>. ROMANIAN RAILWAY AUTHORITY - AFER, ROMANIA

**ABSTRACT:** The railway vehicles are characterized by the fact that the wheel axle moves in the path of travel and self guidance in the contact forces between the tire rim and wheel tracks. Following wheels, besides the three common features they have and other land vehicles, namely support vehicle vertically, running about and propulsion, respectively braking railway vehicles in addition their specific function, namely self guidance that the two wires inside of rail. Being metallic wheels and also the rails that give the vehicle the ability to rail loadings much higher than other land vehicles. This capability, combined with that of self guidance, creates the possibility of forming convoys of vehicles (trains) heavy, giving wheel system - advantages of high capacity rail transport. The study and thorough understanding of the complex phenomena of the contact wheel - rail is actually the fundamental problem that ensures the development of railway vehicles.

**KEYWORDS:** railway vehicles, wheels, rail, teratology

### INTRODUCTION

At the movement of vehicles in curves by constant speed, the points of contact between wheel and rail interaction forces arise from quasi-static, whose value depends on the vehicle and external forces that determine the speed also position of the vehicle once. By entering vehicle dynamic variation curve means determining quasi-static interaction forces between rail and wheel curve by velocity.

The specific resistances at the advance have low values because the wheels rolling on the rails, which determine the specific energy consumption, reported in units of mass of a tonne, transported more than all other land transport systems. However, the ability of rail vehicles self guidance offers the ability to run at operating speeds required in a fully safe and almost independent of the state of the atmosphere and seasons.

The determination of the driving forces of the rim lip also rail guidance forces (leading) angle of the wheel rim also the wire path factor flange wear and rail safety against derailment criterion, transverse force on the bogie frame are taking account of the fact that the values of these parameters must not exceed certain limits set by standards. Thus, one can determine the maximum speed the vehicle can travel through a given radius curve without a danger of derailment, damaging the railway line, or excessive wear of the tires lip wheels and rails leading. To simplify the calculation of the forces driving points, simplifying assumptions are made. Of these assumptions, primarily requires that tread tires to consider cylinder and the friction between the tire also rim neglecting rail. Also, it is considered that the rails also the wheels are new and therefore it is the two-point contact (A - support B - Drive), Ni forces that occur in the driving points B and driven by a common normal of the two contact surfaces, horizontal components are replaced by the equilibrium equations are introduced Pi forces called guiding forces (driving forces).

Not the least bear in mind that advance the attack  $b$  to neglect also to consider the driving forces acting on the vertical plane of the axle, constant velocity is considered not to be taken into account traction or braking forces (considered free movement, resulting in a maximum value of  $P_i$ ). Also, wheel loads are considered equal to  $Q_0$  static, so the pole of rotation axis is bogie path is considered perfectly circular, by constant super elevation and also expansion of the railway line.

Due to actual execution conditions also wheelset assembly center of gravity is not located exactly on the axis of rotation, also one of the principal axes of inertia of the wheelset, which should strictly coincide with the axis of rotation deviates from that.

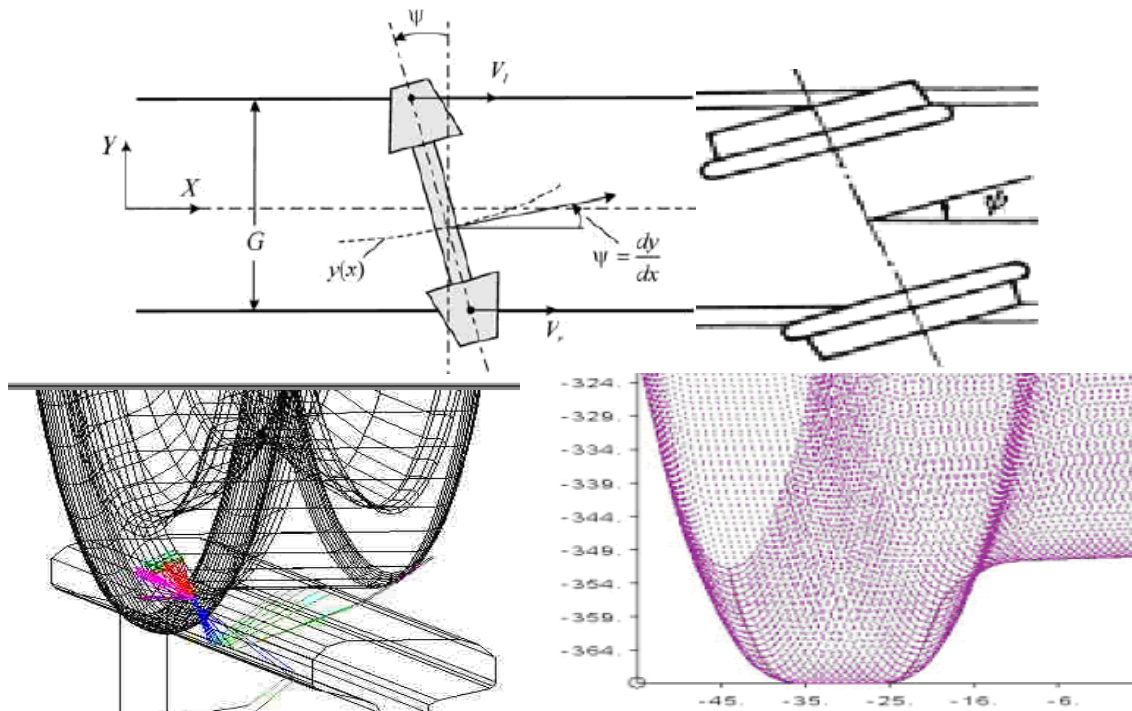


Figure 1. Representation of the angle of attack  $\psi_0 = 7 \cdot 10^4$  mrad

**THE MATTERS OF THE TRIBOLOGICAL PHENOMENON OF WHEEL - RAIL CONTACT**

At action of the wheelset in uniform rotation, centrifugal inertia forces the system is not in balance. In such circumstances it is said that the wheelset is unbalanced. In Figure 2 is the rectangular coordinate system  $Oxyz$  which is related to the forces acting on the wheel and its contact with the track rail. The coordinate system is oriented so that its  $z$ -axis coincides with the axis of the axis of rotation. Axle mounted to rotate around the axis by angular velocity  $\omega$ . The center of gravity  $G$  of the wheelset is not in that situation rotation axis  $Oz$ . Also, the main axis of inertia does not coincide with the axis of rotation.

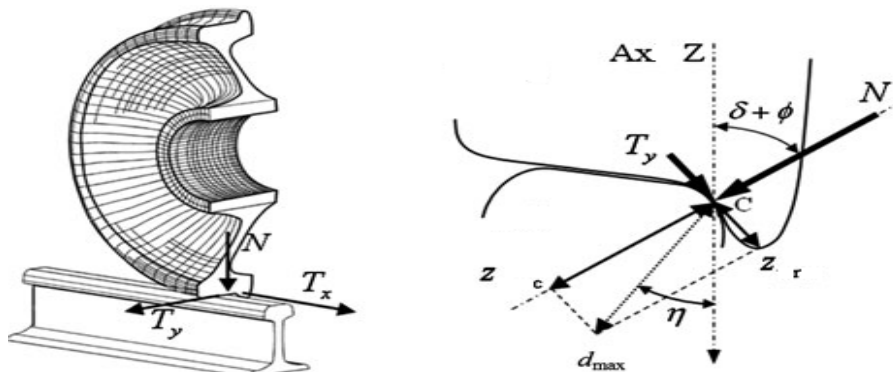


Figure 2. The loading wheelset forces

The main causes that lead to dynamic imbalance are described at length the heterogeneity of the materials were carried wheel set pieces of machining processes (rolling, forging, cutting, etc..) Layout with deviations wheel set subassembly components, deviations from cylindrical assembly components, assembly areas without coaxiality assembly components to the running surfaces of the wheels, and more. Due to their inertia forces system is in balance, it produces a resultant force  $F_i$  and a resultant moment  $M_i$  that, assuming the reduction in the origin  $O$  of the coordinate system, have the next values:

$$\underline{F}_i = m\omega^2 x_G i + m\omega^2 y_G j \tag{1}$$

$$M_i = I_{yz}\omega^2 i + I_{xz}\omega^2 j \tag{2}$$

In the previous expressions, besides already mentioned notations,  $i$  and  $j$  are unit vectors  $Ox$ ,  $Oy$  respectively,  $m$  is the mass of the wheel set.  $x_G$  and  $y_G$  are the coordinates of the center of gravity. Also  $I_{xz}$  and  $I_{yz}$  are the moments of inertia of the wheel set centrifugal different from zero because of inertia axis does not coincide with the axis  $Oz$ . To retain the wheel set bearings in these reactions occur  $R_1$  and  $R_2$ :

$$R_1 = X_1 i + Y_1 j \tag{3}$$

$$R_2 = X_2 i + Y_2 j \tag{4}$$

In the above relations, the factor  $L$  is the distance between the supports resulting in dynamic equilibrium conditions of the axle body which is rigidly mounted. Sizes the reactions  $R1$  and  $R2$ , which supports loads are dependent on the eccentricity of the center of gravity  $G$  with coordinates  $x_G$  and  $Y_G$ ,  $I$  wheel set mass, moments of inertia and centrifugal  $I_{XZ}$   $I_{yz}$  and angular velocity  $\omega$ .  $R1$  and  $R2$  reactions, whose components are given by the expressions (5) and (6) are fixed in the coordinate system  $Oxyz$ , related to the wheel set.

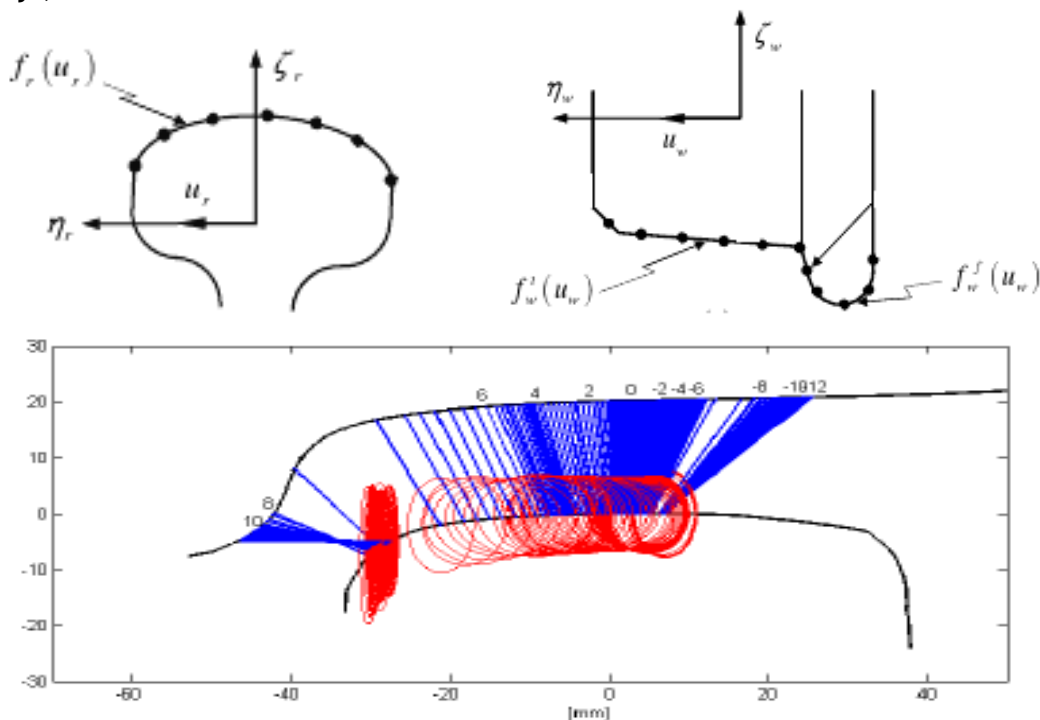


Figure 3. Highlighting the tensions that occur in the area of the wheel - rail contact

Conventionally, a rigid body mass rotation is considered if the frequency of rotation is 0.7 in the lowest characteristic frequency of vibration. To balance the wheel sets on dynamic balancing machines to determine, in a specific machine, balancing masses  $ME1$  and  $ME2$ , which is extracted in balancing plans I and II, as shown in Figure 3 so that the centrifugal forces produced  $E1$  and  $E2$ , together with the forces of inertia of the wheel set, be in balance and reactions  $R1$  and  $R2$  be void. In this way the center of gravity  $G$  of the wheel set in the draw material is brought to the rotation axis and the main axis of inertia is superimposed on the axis of rotation  $I_{xz} = I_{yz} = 0$ .

Through a balancing by extraction of material in a single plane can not cancel only the resultant inertia forces remaining  $F_i$  when my inertia forces given by (2). This is the static balance. This is to bring the center of gravity to the axis of rotation, the axis of inertia but does not overlap with the axis of rotation. Reaction of supports is not canceled. In their values given by equations (5) and (6), the remaining terms containing the  $I_{XZ}$  and  $I_{yz}$ , which are different from zero. To finish balancing in this case must be canceled and the moment of inertia  $I$ , by withdrawing forces mass balance. The imbalance dynamic wheel set can be characterized quantitatively by product  $D_z = m \cdot e$ , where  $m$  is the mass of the wheel set and  $e$  is the eccentricity of the center of gravity from the axis of the wheel set. The product  $m \cdot e$  may indeed be admitted largest imbalance characterizing dynamic wheel set as a rotating centrifugal force produced in the body is  $F_c = m \cdot e \cdot \omega^2$ , in witch case  $\omega$  more than the angular velocity. As the imbalance  $D_z = m \cdot e$  is greater than the centrifugal force is greater at the same angular velocity.  $D_z$  The imbalance magnitude can be used as a comparison for balancing quality wheel sets of the same kind, that is the same shape, same size, same material and thus the same weight and its distribution.

For different wheel set mass, even in the same category of rolling stock, size  $D_z$  can not be adopted for comparison. Meanings are more complete mass eccentricity, calculated by dividing the mass imbalance  $D_z$  wheel set which is of the form  $e = m \cdot e / m$ , measurable in (g.mm/kg) or  $\mu\text{m}$ . This size is, as it turns out, the physical significance of eccentricity. This size is adopted to characterize the degree of balancing of wheel sets. Acceptable values are standardized for mass eccentricity. In a class of quality in determining the permissible mass eccentricity ( $e$ ) has been considered experimental finding that for a similar dynamic behavior is necessary with increasing speed in work value is to be kept small. They admitted that, for the same class, the product  $e \cdot n = ct.$  or  $e \cdot \omega = ct.$  The  $E \cdot \omega$  value of this constant is the fundamental characteristic of a class of quality. All the forces acting on the vehicle is considered in the plane tangential to the road surface. The way the vehicle is considered non-deformable flat. Frictional forces between the wheel tread and rail wheel load dependent,

Coulomb forces can be considered, by constant friction coefficient according to Heumann's theory with a friction wheel according pseudo sliding but isotropic according to Lévi, Müller also the ORE Committee.

The anisotropic friction coefficients shall be elected by longitudinal and transverse direction, considering pseudo sliding tangential forces  $T_x$  also  $T_y$ , as Kalker theory. For example, in calculations to consider locomotive BR 189 (Figure 4).

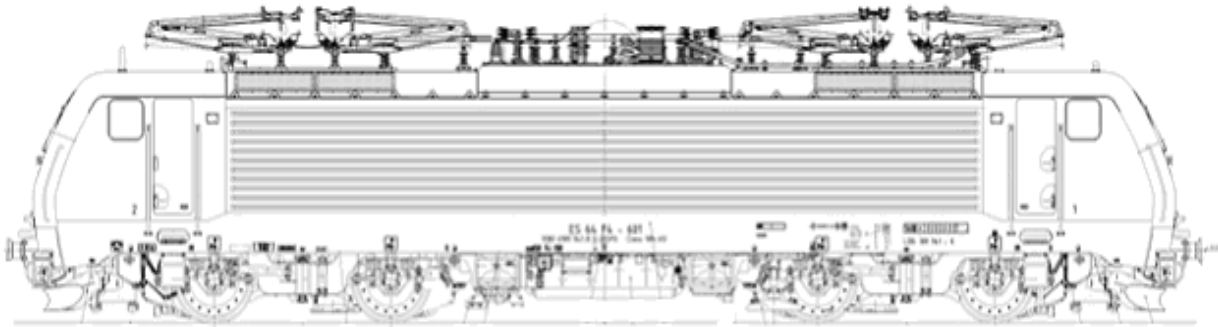


Figure 4. The four-axle electric locomotive BR 189 Class

It was considered the first bogie of the locomotive BR 189 (Figure 5) during the movement of the curve, by forces and moments acting on it. The second bogie is not represented, but it may deem it to be in the mirror to the first.

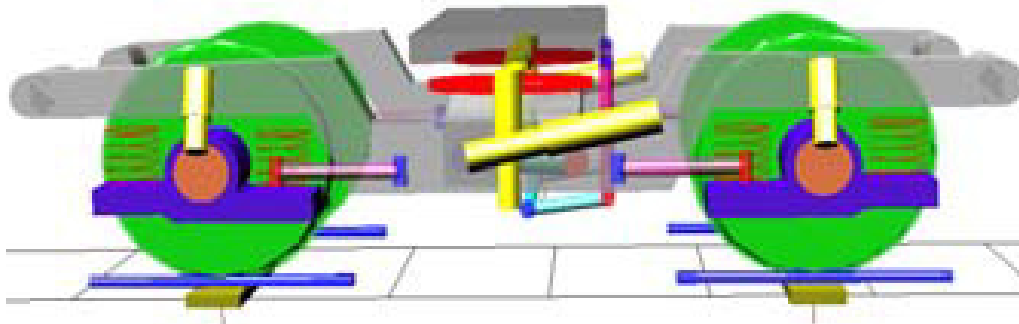


Figure 5. The four-axle bogie of BR 189 Class electric locomotive

For the systematization of the calculations, the parameters related to a coordinate system  $xOy$ , positive sense of forces and moments which is indicated in Figure 2. FFI and friction forces are represented by the coefficient of friction in the case isotropy. If the treaty is not taken into account the coupling between bogies also will follow their behavior in the free state. The movement of free bogies in the curve railway line is independent. There is a time booster ( $M_r \neq 0$ ) also hence a imposed on velocity, the two bogies are disposed differently from the yarn path also at the same time it is necessary to analyze the movement of the two bogies.

It is considered that the first bogie of the locomotive forces acting  $P_i$ ,  $C$ ,  $F_v$ , FFI (hypothesis isotropy friction, but the coefficient of friction varies), and when  $M_r$ . Since, in terms of speed, the vehicle can travel in principle all three positions characteristic calculation aims to determine the speed variation by forces  $P_1$  also  $P_3$ , respectively  $Y_1$  also  $Y_3$ , gear shift position bogie variation polar distance  $p$ , the angle of attack  $\alpha$  and wear factor  $\varphi$ .

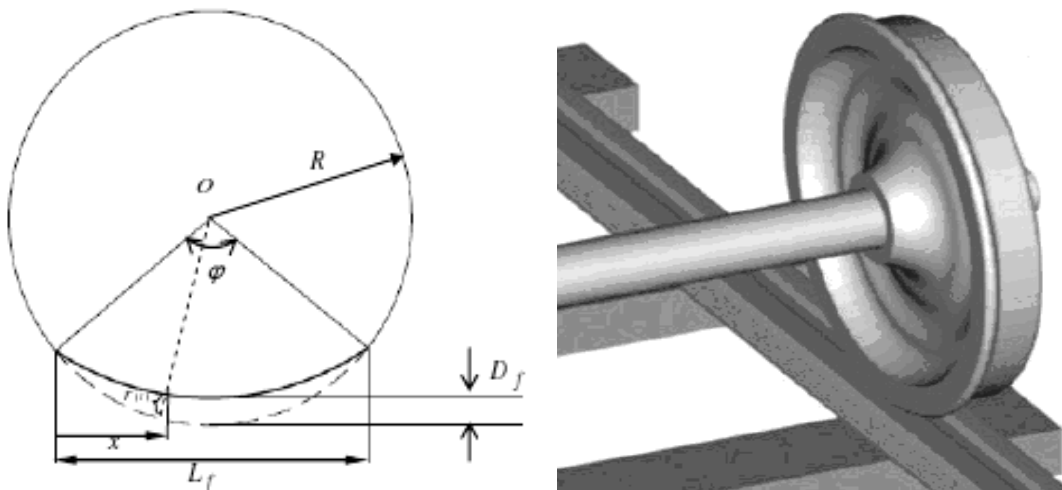


Figure 6. The simulation of the plan place

Normally newly created site plan (Figure 6) has a length of approx. 50 mm and can reach 100-120 mm. At first, the site plan is shaped chord (seen in radial section of the wheel) but then the edges are rounded place plan due to wear. Location plan with rounded edges is called instead plan worn or rounded plan instead. To calculate the relative displacement wheel instead plans - the influence of place rail plan is tantamount by a hollow profile rail longitudinal fungus, considering both perfectly round wheels. In the case of place plan used, the edges are rounded and therefore equivalent rail profile consists of two arcs connecting parable also a means arc corresponding place plan. Due to wear at the edges and flattening, place plan length used is longer than the place from which new plan. Applying a numerical simulation, it is observed that due to curvature sensitive wheel, differences between plans also profile equivalent of place relative displacement wheel - rail that is input into the system wheel - rail when simulating shock given the location plan. A discontinuity between wheel tracks that is required is you cross the discontinuity of the right locking joints is considered to be the most severe. If the shock by wheel passes more than a rail joint, the excitation system wheel - rail is caused also by the relative displacement between wheel and rail which cover particular aspects. It starts from the longitudinal profile of track modeled by arcs of a parabola and calculate the wheel path. When the wheel has arrived in the center of the joint, there is double contact (bicontact) longitudinal rail and the trajectory of the wheel is turning back, which is indicative of the instantaneous variation in the speed of the vertical component of the dynamic system conditions. Results in a variation of the instantaneous vertical component of momentum wheel and shock load so infinite elasticity assumption that it neglects the path. In reality, the wheel passes more than joint no such change of momentum due to the elasticity of contact. Wheel path is smooth, continuous slope. It also takes into account the Hertz nonlinear type. It is thus more accurate estimate shock force highlighting unloading rail behind the wheel, while the front rail loading.

The analysis the general case in which the joints are leveling gap and difference involves studying three situations that can bridge the gap joints wheel namely that tangentially bicontact, mono tangentially also non tangentially. Due to the influence of the radius of the wheel, the wheel is less than that required by contact with the rail and the wheel is continuous and smooth trajectory as a result of the introduction of elastic bicontact. In this context we review an analysis of the geometry of a perfectly round wheel also a corrugated rail running surface (Figure 6.a) either sinusoidal or after a certain law. Numerical application developed is intended to illustrate the radius of curvature of the travel wheel relative to the wheel - rail. This is accomplished by comparing the relative displacement of two sizes that wheel - rail also rail profile. The difference between the two values increases as the amplitude of the rail profile or the wavelength increase the profile of the rail is smaller. Of course, in the case of large wavelength range, which means the low speed range, the effect is negligible. It becomes relevant for smaller wavelengths as short wave meets the wear of the rail.

The influence the radius of curvature of the wheel relative displacement of wheel - rail is likely nonlinear geometric effect plus the input mechanical contact, as we shall see in the following sections. As a result, the range of relative movement of the wheel - rail has a single part corresponding to the light, but many. It should be noted there is also a fundamental component is less than the roughness of the channel. The amplitude of the first harmonic due to the effect of the radius of curvature of the wheel depends on the roughness of the amplitude and the wavelength thereof. The amplitude of the first harmonic amplitude increases non-linearly with roughness, and this increase is more pronounced when the wavelength reduction. On the other side, it is found that the radius of the wheel play an important role. Larger diameter wheels give a more geometric effect. In general, the drive wheels are constructed by a larger diameter than the non engines. In addition, it is noted that tread wear is more intense when running a wheel traction motors developing. Corroborating the two aspects mentioned that the effect of the beam geometric wheel could play a significant role in the initiation, especially in developing wave rail wear. Geometry The analysis wheel - rail by some highlights waviness nonlinearities increase relative displacement amplitudes of the spectral components of wheel - rail according to amplitude undulations.

#### **THE STUDY OF THE CONTACT PRESSURE AND RIGIDITY OF WHEEL - RAIL CONTACT**

The tribology of wheel - rail contact type informally, means that the footprint is in the tread of the wheel also rail cross sections where the radii of curvature are much larger than the size of the contact patch in the presence tread irregularities. Problems of contact between two solid bodies know two things that normal matter tangential issue. The normal problem is starts from the geometrical shape of the bodies and determines the size of the contact patch, normal contact pressure distribution and the relationship between bodies also near normal contact force. Within the problem of tangential contact tangential pressure distribution interests also friction forces with the starting point of a body sliding speeds also normal problem results. In the general case, the two points are connected, but in certain circumstances they may be treated separately, as is otherwise the case of the system the wheel - rail. With the wheel - rail contact model assumptions are valid nonformal

Hertz relations. This issue are presented for the computation of contact ellipse semi-axis size, contact pressure also contact rigidity of.

These parameters affect tread wear also dynamic wheel - rail. The contact ellipse dimensions and distribution of contact pressure changes due to undulations tread. The numerical simulation performed for a wheel (Figure 1) with a profile UIC 60 rail wear, by highlighting the contact rigidity of nonlinearities depending on the load on the wheel contact ellipse dimensions shows that when the rail running surface a sinusoidal waviness varies as follows: the ellipse along the axis of the track groove is increased to reduce ripple also the ripple at the top, while the major axis of the ellipse of contact, which is oriented perpendicular to the rail, has an opposite variation, that is, ripple contracts and expands into the recess at the top of the ripple undulation [6].

Furthermore, it is noted that large semi-axis varies less than the other also, as a result, variations also changes will dictate smaller semi-axis of the contact area. As a result, the maximum contact pressure will change semi-axis against the variation along the track, that is, the maximum pressure recorded when the wheel is located on top of the ripple, and then, while its side down in the recess, the contact pressure reach the lowest values. Moreover, based on the same results, it is found that the approximation wheel - rail varies similarly to the maximum contact pressure. Finally, it is inferred that the contact stiffness variation is to have a reverse approach, that contact is elastic and stiff peak ripple recess. In general, the wheel is accompanied by the slide rail in the longitudinal direction and transverse direction, and the pivot (spin) due to the rigid attachment of the wheel axle also the reverse taper of the wheel tread profiles. Furthermore, movement in the drive axle or brake to intensify the longitudinal slip. These slides are provided for moving the axle like a rigid body also may be described by the speed of sliding, a concept known in the literature as creep.

The ratio between sliding speed due to axle considered rigid body movement also roll speed axle that pseudo sliding called creepage. The contact ellipse slides appear elastic. With by axle load tasks in vertical and horizontal planes, the contact area, in addition to the normal stresses, shear stresses develop distributed totaling give friction also friction moment pivot (spin). Contact ellipse is divided in two areas, an elastic deformation occurring only called adhesion area, also the other in the certain area of the sliding slides occur. In the case of the contact ellipse are two sides of it are respectively front and rear edge. When a particle enters through the front edge of the contact ellipse it go from undeformed (unaltered) to the deformed due to the transfer of horizontal force between wheel and rail. In fact, the particle is subjected to shear stress also as long as this voltage is lower than the voltage limit given by the normal voltage tangential multiplied by the coefficient of friction is in the bonding particles. As the particle moves away from the front edge, also tangential strain increases so that that becomes equal to the tangential limit, at which, according to the law of friction, the particle enters into the slip.

The essence of the problem tangential wheel - rail contact is to establish the correlation between pseudo sliding, the contact normal force also friction force. It should be noted that the current speed locomotives that hauled trains for passenger transport (as is the case locomotive class BR 189 - Figure 4) are constructed starting regime is more extended to speeds of approx. 100 km / h also more. During this procedure, electric traction motors are so adjusted as to operate at constant torque which means the drive at the limit of adhesion when the value reached pseudo sliding are important. For the evaluation of mechanical work consumed by friction only be understood sliding the related area. To calculate the work is therefore necessary to know the footprint divided into the two areas.

For the analyzed case, the driving wheel of a locomotive BR 189, to calculate the contact ellipse, by demarcation of areas of adhesion and sliding. It is noted that the differences in the sliding groove when the wheel is in ripple compared by the situation when the wheel is at peak ripple. In that paper, we tried to identify a new model of the rail support system consists of three Kelvin - Voight [3] that models correctly oriented three-way stand rail way inhibit bending wave propagation by limiting rotation of the right rail sleepers sections (Figure 6).

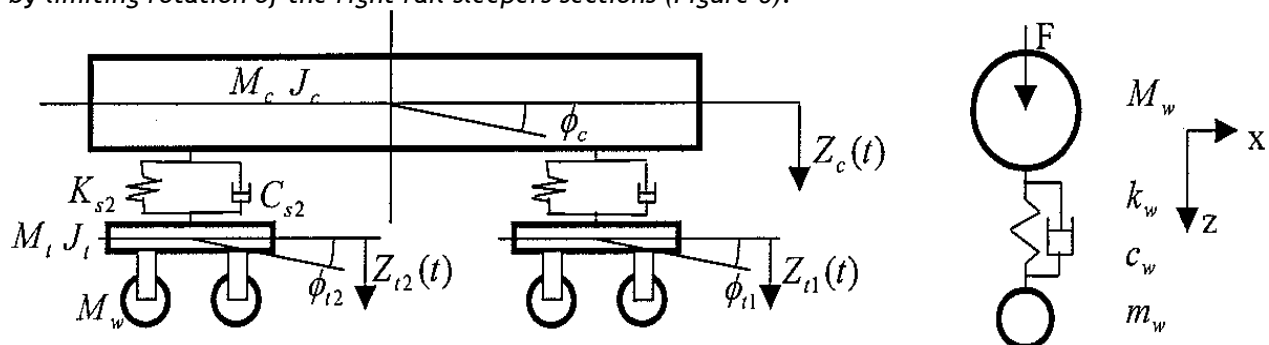


Figure 6. The Kelvin - Voight rheological model of the BR 189 class locomotive suspension'

Another problem is the rail response at low frequencies, below 50 Hz. Instead resonance reported for harmonic force excitation by fixed support, there are two resonances whose frequencies with the resonant frequency of the force given fixed form an arithmetic progression support. This makes the speed increases, responsive rail to fall and this is likely to influence the size of the forces of wheel - rail contact also the appearance and development of rail wear wave. The Green matrix method path is extended to study the response and then track the action moving harmonic forces. The Green Matrix Green matrix of direct and conjugate [6] allow highlighting displacement rail components under the action of harmonic forces mobile. Comparing himself to answer a harmonic force by mobile phones harmonic response to two forces at a distance equal to the bogie wheelbase, numerical simulations show significant differences between the two cases.

## CONCLUSIONS

The calculation of the frictional force shall be made starting to the relationship in the literature, and then they are completed so that the study is centered only for longitudinal sliding of particular interest in the problem of vibration axles under the starter motor. Edifying results are obtained on the basis of numerical simulation by application to a driving wheel having contact with a conical profile UIC 60 rail showing a waviness in the tread. Thus, it is noted that the wheel velocity influences the coefficient of friction in order to reduce it to higher pseudo sliding 2 - 3 %. The growth rate coefficient of friction at zero pseudo sliding higher undulation ripple when the wheel is in recess. The coefficient of friction is greater the greater part of the sliding pseudo range considered for simulation.

For the pseudo sliding greater than 4 - 5 %, the coefficient of friction is not influenced by the position of the wheel on the track undulation. The results of calculations made for the case in which the profile of the wheel is concave shown that, in general, the same issues remain in the sense that the relative speed reduces the coefficient of friction, and on the other hand, the coefficient of friction is greater more than the wheel tread ripple recess until it is on top of it. Finally, it should be noted that in the case of concave profile, the friction coefficient is higher. Depreciation is a consequence of the process of friction also is detachment from material and modifying the initial state of the contact surfaces, the wheel - rail is one such rigid.

At frequency drops below 50 Hz, according to experimental results, receiver rail increases, and this can not be achieved by current models. He also noted the fact that if the inertial effect of the ballast is introduced by a rigid block by one degree of freedom, the rheological properties of ballast systems can be modeled by three Kelvin - Voigt oriented three-way and the embankment can be further shaped by a Kevin system - Voigt in parallel with a Maxwell. Actual The Green functions themselves represent its response to a unit impulse force applied to a point in a certain section of the track. Real The Green functions [6] are calculated numerically by applying the Fourier transform, inverse The Green functions defining complex undulation function. With real The Green function matrix is assembled that describes the response The Green rail track along the distance between the two rails to power boost mobile unit. The Green Matrix path is periodically alleviated in time and space and allows simulation of the rail response to a harmonic force mobile. Analyzing the dynamic response of rail under harmonic force furniture is made to show the influence of the Doppler effect [6] in the resonant periodic support rail on sleepers.

It is pointed out that the natural frequency of the system axis - a running path is between 30-60 Hz and for the separation of the beams to 0.6 m, the frequency of resonance occurs at a speed of 18-36 m / s, or 65-130 km / h Important results of the parametric study of vibration motors to the axles of high-speed trains during the start-up procedure for both traction control system performance, as well as problems of wear of the tread. Furthermore, the variable component is responsible for the occurrence of wear and tear wave. It should also be added that the wear is produced in the sliding contact patch but not in the area where there is no relative movement adhesion between the wheel and the rail. The maximum width of the slip zone increases linearly by frequency response pseudo sliding also treads [6]. Vibration characteristic of this scheme is that it modifies the response itself as force is applied between the rails or right of railway sleepers.

Whether the excitation force is applied between the railway sleepers, rail has a resonant frequency located approx. 1070 Hz for rail UIC 60 on railway sleepers placed at 60 cm from each other. If the excitation force is applied in front of railway sleepers when the vibration of the rail system is marked by an anti resonance frequency located at a higher value than the resonance (ca. 1100 Hz for the case mentioned). There is one major problem, namely, Euler beam model rail type - Bernoulli is not suitable for resonant frequencies - anti resonance calculated are much higher than those obtained experimentally. As a result, the Timoshenko beam pattern must be used which take into account the effect of the force of rotation of the cutting section as well as the inertial effect of the rotation of the beam sections.

## REFERENCES

- [1] BEYNON, J.H., BROWN, M.W., DWYER-JOYCE, R.S., KAPOOR, A., LO-MORREY, M., GIEVE, D.G., and FLETCHER, D.I., "Integrated Study of Fatigue and Wear of Pearlitic Rail Steels Under Rolling - Sliding Contact Conditions", Proc. 5th Int. Conf. on the Contact Mechanics and Wear of Rail/Wheel Systems 'CM2000', Tokyo, Japan, pp. 104-108;
- [2] BURSTOW, M. C., WATSON, A. S. and BEAGLES, M. (2003) Simulation of rail wear and rolling contact fatigue using the Whole Life Rail Model. Proceedings of 'Railway Engineering 2003', London 30th April-1st May 2003;
- [3] DUMITRU, G. "Trenuri de mare viteza" (Trains For High Speed). Revista MID-CF (MID-CF Gazette), no. 5/2008
- [4] EVANS, J. R. (2003) Dynamic Modelling of Rolling Contact Fatigue, AEATR Report, AEATR-VTI-2003-048, July 2003;
- [5] HEUMANN, H., "Grundzüge der Führung der Schienenfahrzeuge", Olandenburg - Verlag, 1954.
- [6] MAZILU, T., "Vibrații" (Vibrations), Editura Matrix Rom, București, 2012.
- [7] RINGSBERG, J. W. and JOSEFSON, B. L. (2000) Finite element analysis of rolling contact fatigue crack initiation in railheads, J. Rail and Rapid Transport.
- [8] ORE B55 RP1, Recomandations relatives aux dispositifs de mesure les plus convenables et aux tolerances admissibles;



ANNALS of Faculty Engineering Hunedoara



- International Journal of Engineering

copyright © UNIVERSITY POLITEHNICA TIMISOARA,  
FACULTY OF ENGINEERING HUNEDOARA,  
5, REVOLUTIEI, 331128, HUNEDOARA, ROMANIA  
<http://annals.fih.upt.ro>